Natural Variation in a Chloride Channel Subunit Confers Avermectin Resistance in *C. elegans*

Rajarshi Ghosh, Erik C. Andersen, Joshua A. Shapiro, Justin P. Gerke,* Leonid Kruglyak†

Resistance of nematodes to anthelmintics such as avermectins has emerged as a major global health and agricultural problem, but genes conferring natural resistance to avermectins are unknown. We show that a naturally occurring four–amino-acid deletion in the ligand-binding domain of GLC-1, the alpha-subunit of a glutamate-gated chloride channel, confers resistance to avermectins in the model nematode *Caenorhabditis elegans*. We also find that the same variant confers resistance to the avermectin-producing bacterium *Streptomyces avermitilis*. Population-genetic analyses identified two highly divergent haplotypes at the *glc-1* locus that have been maintained at intermediate frequencies by long-term balancing selection. These results implicate variation in glutamate-gated chloride channels in avermectin resistance and provide a mechanism by which such resistance can be maintained.

A vermectins are secondary metabolites of the cosmopolitan soil bacterium *Streptomyces avermitilis* (*1*) that are used for management of agricultural and parasitic nematode infestations. Abamectin (a mixture of avermectin B1a and B1b) is an agricultural pesticide, and ivermectin (a synthetic derivative of avermectin B1a and B1b) is a veterinary and human anthelmintic (*2*). Responses to avermectins by nematodes are thought to be dependent on a diverse set of molecules, including glutamate-gated chloride channels and P-glycoproteins (*3*). Widespread resistance of nematodes to these drugs is a global concern for agriculture and health (*4*), but the genetic basis of natural resistance to avermectins has remained elusive (*4*, *5*).

To investigate the genetic basis of natural avermectin resistance, we used a swimming assay (*6*) to quantify the ability of avermectins to induce paralysis (*7*) in strains of the nematode

Caenorhabditis elegans isolated from different geographical locations. We found that a Hawaiian wild isolate of *C. elegans*, CB4856, was resistant to abamectin and ivermectin, while the laboratory strain, N2, was sensitive under identical conditions; for example, exposure to 0.5 μg/ml of abamectin for 30 min resulted in paralysis of 98% of N2 worms but only 17% of CB4856 worms (Fig. 1, A and B, and figs. S1A and S2). As a comparison, ivermectin reduces worm load by 100% in cattle infected with ivermectin-sensitive parasitic nematode *Cooperia oncophora* and by 70% in cattle infected with ivermectin-resistant *C. oncophora* (*8*). F1 heterozygotes from reciprocal crosses between N2 and CB4856 were as sensitive to abamectin as the N2 parent (Fig. 1, A and B), which suggests that abamectin resistance may be a recessive trait caused by a loss-of-function allele in CB4856.

To identify the gene(s) responsible for the observed difference in abamectin response, we carried out quantitative trait locus (QTL) mapping in a panel of recombinant inbred advanced intercross lines (RIAILs) generated from crosses between the N2 and CB4856 strains (*9*). We measured the frequency of body bends, as well as the probability of animals being paralyzed after 30 min in 0.5 μg/ml abamectin, for 210 RIAILs. The traits were not normally distributed and were significantly correlated with each other (fig. S3A). Nonparametric interval-mapping (*10*) for all measures of response to abamectin revealed a major QTL on chromosome V (Fig. 2A and fig. S3B). RIAILs bearing the CB4856 allele at this locus exhibited higher mean frequency of body bends and lower probability of being paralyzed after 30 min of exposure to
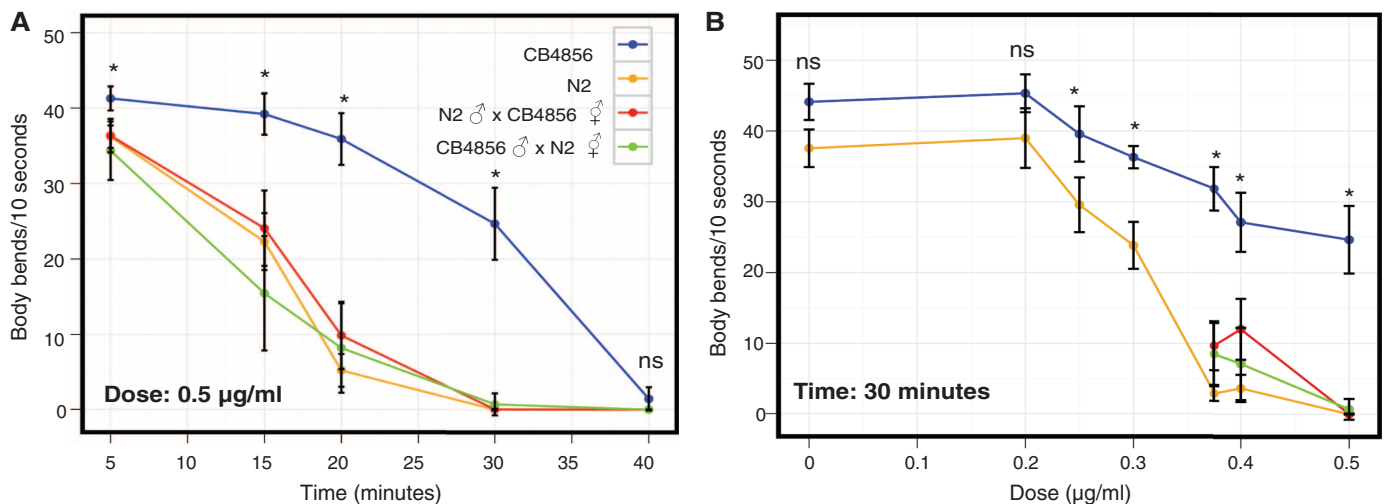
Lewis-Sigler Institute for Integrative Genomics, Department of Ecology and Evolutionary Biology, and Howard Hughes Medical Institute, Princeton University, Princeton, NJ 08544, USA.

*Present address: Pioneer Hi-Bred International, A DuPont Business, Johnston, IA 50131, USA

†To whom correspondence should be addressed. E-mail: leonid@genomics.princeton.edu (L.K.)

Fig. 1. Sensitivity to abamectin differs between N2 and CB4856. (**A**) Time course of frequency of body bends ($n \geq 20$ animals for each strain). *, significantly different from CB4856 ($P < 0.01$). The legend depicts the strains and their respective colors in (A) and (B). (**B**) Frequency of body bends at 30 min plotted against different doses of abamectin for N2 (orange, $n \geq 12$ animals at each dose); CB4856 (blue, $n \geq 12$ animals at each dose); F1 progeny from crosses between N2 males and CB4856 hermaphrodites (red, $n \geq 18$ animals at each dose); and F1 progeny from crosses between CB4856 males and N2 hermaphrodites (green, $n \geq 28$ animals at each dose). Heterozygotes were scored only at 0.375 μg/ml, 0.4 μg/ml, and 0.5 μg/ml abamectin. Error bars, mean ± SEM for each strain. ns, nonsignificant difference. *, $P < 0.01$. P values are from Mann-Whitney tests for concentrations of 0 to 0.3 μg/ml. For the higher concentrations, where more than two groups were involved, a Kruskal-Wallis test followed by Dunn's multiple comparison test was performed.

abamectin (Fig. 2C), but not all RIAILs with this allele were resistant, which suggests that additional loci are likely involved. Analysis of abamectin response as a binary trait (6) revealed a second QTL on chromosome III (fig. S3, C and D). Joint QTL analysis of the loci on chromosomes V and III indicated that they act additively and explain ~26% and ~6% of the phenotypic variance, respectively (6) (table S1).

Genotyping of additional markers in RIAILs followed by transgenic rescue with fosmids identified an 11.4-kb segment of N2 DNA that abolished abamectin resistance in CB4856 (Fig. 2, B and D to G, and fig. S5, A to C). This region contained six genes, one of which, glc-1, encodes the alpha subunit of a glutamate-gated chloride channel (11–13), a known target of avermectins (11, 12). A 4.5-kb N2 genomic fragment containing two genes, including glc-1, significantly reduced abamectin resistance of CB4856 (Fig. 2, F and G, and fig. S5D), supporting glc-1 as a candidate causal gene. Crossing CB4856 with the glc-1(pk54) mutant strain, which harbors a pre-

sumptive loss-of-function allele of glc-1 in the N2 background (12), resulted in F1 progeny resistant to abamectin, in contrast to F1 progeny from crosses between N2 and glc-1(pk54), which were sensitive (Fig. 3A). Introgression of the glc-1 region from N2 into CB4856 restored sensitivity to abamectin, whereas introgression of this region with the glc-1(pk54) mutation resulted in abamectin resistance comparable to CB4856 (Fig. 3A). These and additional results (6) (fig. S4) are consistent with a loss-of-function CB4856 allele of glc-1 conferring abamectin resistance in this genetic background (6).

To identify the underlying functional polymorphism(s), we sequenced the N2 and CB4856 alleles of glc-1. Relative to N2, CB4856 had 77 single-nucleotide polymorphisms (SNPs) in the coding region, 32 of which resulted in amino-acid changes, as well as a four-amino-acid deletion in exon two (fig. S6A). Despite the multiple coding polymorphisms, the predicted secondary structure and membrane topology of GLC-1 from N2 and CB4856 were similar (6) (fig. S6, B

and C). Alignment of the predicted structure of CB4856 GLC-1 with the three-dimensional structure (14) of homomeric GLC-1 bound to iver-mectin and glutamate revealed no obvious changes in the overall structure of GLC-1 (fig. S6C). Based on structure and annotation, we selected three candidate polymorphisms for further analysis. A threonine-to-alanine substitution at position 346 may weaken binding to avermectins by eliminating one of three hydrogen bonds between GLC-1 and ivermectin (fig. S6C), an alanine-to-threonine change at position 20 may reduce the cleavage probability of the signal peptide (6), and a four-amino-acid deletion in the ligand-binding domain of GLC-1 may interfere with the kinetics of glutamate binding. Comparison with the closest homolog of glc-1 in C. elegans, avr-15, showed that the CB4856 deletion allele is likely derived (fig. S7A).

To determine whether any of these polymorphisms confer resistance to abamectin in CB4856, we transformed CB4856 with N2 glc-1 cDNA constructs driven by a 1.1-kb glc-1 promoter,
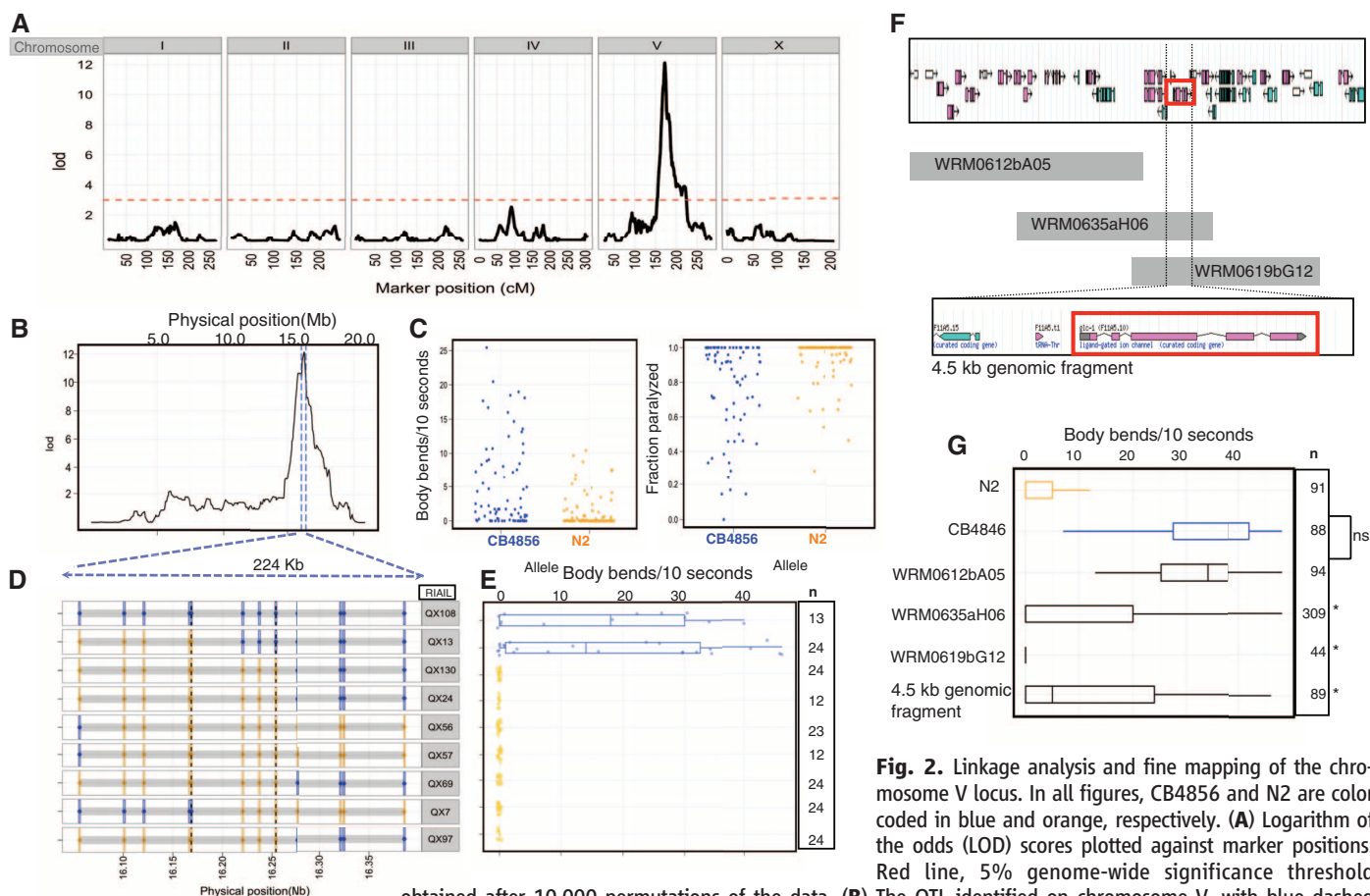

Fig. 2. Linkage analysis and fine mapping of the chromosome V locus. In all figures, CB4856 and N2 are color coded in blue and orange, respectively. (**A**) Logarithm of the odds (LOD) scores plotted against marker positions. Red line, 5% genome-wide significance threshold obtained after 10,000 permutations of the data. (**B**) The QTL identified on chromosome V, with blue dashed lines showing the 1.5 LOD-drop interval. (**C**) Distribution of trait values of RIAILs grouped by genotypes at the marker corresponding to the maximum LOD score on chromosome V. (**D**) Genotypes of RIAILs with breakpoints within the QTL interval. Vertical bars with dots are genotyped markers. (**E**) Box plots of body-bend frequency of RIAILs. Each dot represents a single individual. (**F**) (Top) 107-kb genomic interval within the QTL on chromosome V. (Middle) Horizontal gray bars depict the region of the genome (upper panel) covered by each fosmid. The bottom pull-out shows the 4.5-kb N2 genomic fragment. (**G**) Box plots of the frequency of body bends in abamectin of parental and transgenic strains in CB4856 background harboring indicated N2 fosmids and a genomic clone. Pooled data of rescue lines for each fosmid or genomic fragment are plotted (individual lines are shown in fig. S3). ns, nonsignificant difference. *, P < 0.001 from CB4856.

separately harboring each of these three sequence changes observed in CB4856. The N2 *glc-1* cDNA induced sensitivity to abamectin in the otherwise resistant CB4856 strain (Fig. 3B and fig. S5, I and J). Similar results were obtained when CB4856 worms were transformed with N2 *glc-1* cDNA harboring the amino-acid substitutions in the signal peptide (A20T) or in the avermectin binding domain (T346A) (Fig. 3B and fig. S5, L to N). However, the construct harboring the deletion in the ligand-binding domain failed to induce sensitivity to abamectin in
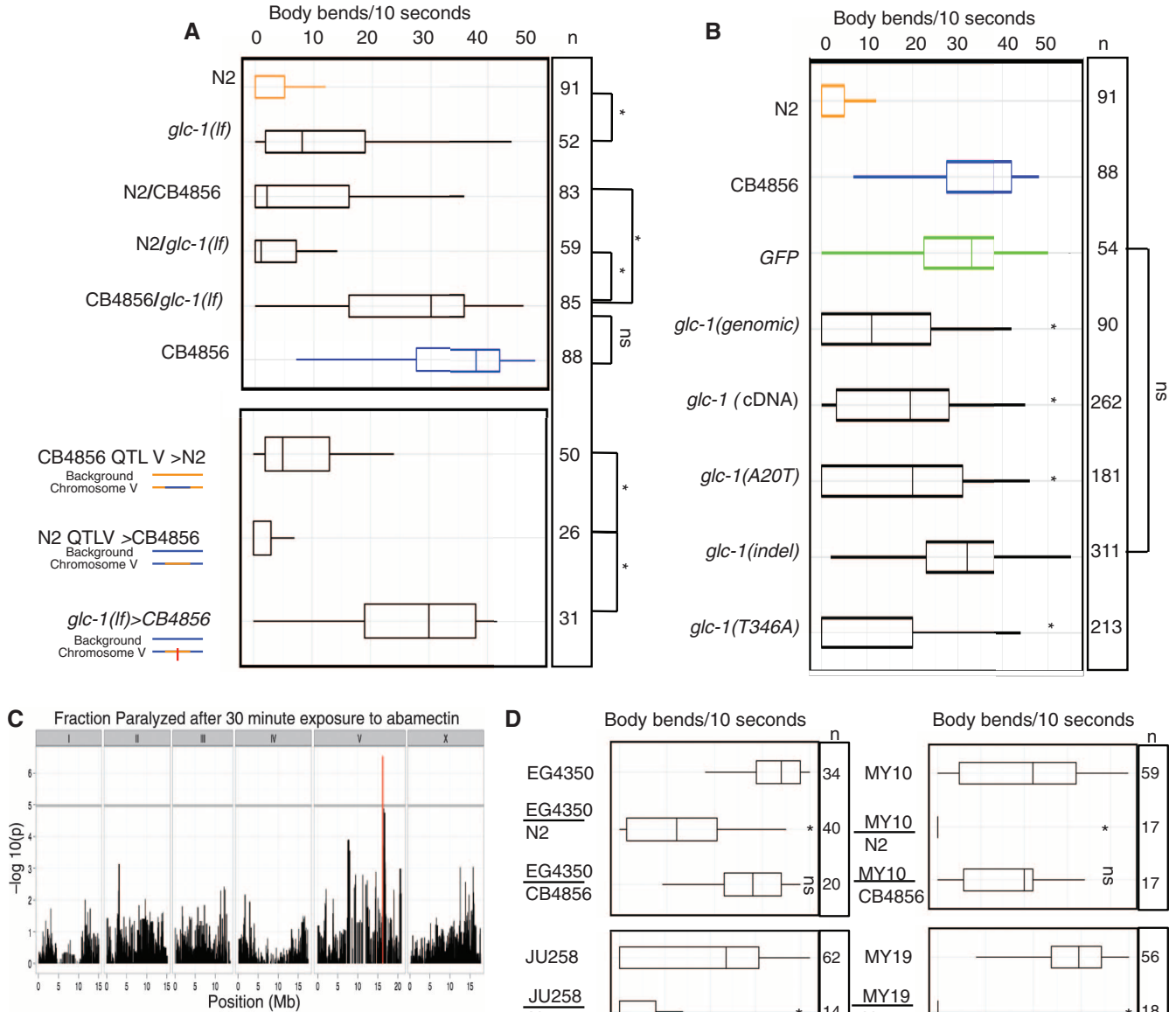

Fig. 3. Common naturally occurring deletion in *glc-1* confers abamectin resistance. In all figures, CB4856 and N2 are color coded in blue and orange, respectively. ns, nonsignificant difference. (**A**) Box plots of frequency of body bends for the indicated strains in abamectin. N2/*glc-1(pk54)* and CB4856/*glc-1(pk54)* are F1 heterozygotes. (Bottom) Introgression strains and their schematic genotypes. The red vertical line depicts *glc-1(pk54)*. *, significantly different (*P* < 0.001) from CB4856. (**B**) Box plots of frequency of body bends for the parent strains [as in (A)] and transgenic strains in the CB4856 background. Green fluorescent protein (GFP), genomic DNA clone of *glc-1*, and the *glc-1* cDNA with and without mutations, were expressed under a 1.1 kb *glc-1* promoter and an *unc-54* 3′UTR (untranslated region). Box plots show pooled data of individual lines shown in fig. S3. CB4856 was transformed with *glc-1* cDNA harboring the following mutations: *glc-1(A20T)*, *glc-1(indel)*, and *glc-1(T346A)*. *, *P* < 0.001 significant difference from GFP. (**C**) Genome-wide association mapping for fraction of worms paralyzed in abamectin. Significantly associated markers (*P* < 3 × 10⁻⁷) are indicated by red lines. (**D**) Box plots of body bends per 10 s in 0.375 μg/ml abamectin are plotted for each wild isolate and the indicated F1 heterozygotes. *, significantly different from the corresponding wild isolate (*P* < 0.01).

CB4856, demonstrating that the four-amino-acid deletion alone is sufficient to generate resistance to abamectin (Fig. 3B and fig. S5K). We cannot rule out the possibility that other polymorphic residues also contribute to abamectin resistance.

A genome-wide association study measuring abamectin resistance in a diverse worldwide collection of 97 wild *C. elegans* isolates identified nine SNPs that were significantly associated ($P < 3 \times 10^{-7}$) with the fraction of worms paralyzed in abamectin (Fig. 3C). These SNPs all fell within a ~47-kb region of linkage disequilibrium that includes *glc-1* (fig. S9). We sequenced *glc-1* in 53 diverse wild isolates and found that 16 carried CB4856-like alleles, including the four-amino-acid deletion, and 37 carried N2-like alleles lacking the deletion. As expected, the presence of the deletion was significantly associated (Pearson's $r = 0.62$, $P <$ 0.0001) with abamectin resistance (fig. S8). However, some isolates with the deletion were sensitive, and some isolates lacking it were resistant, indicating that other genetic factors influence abamectin response. We crossed six resistant wild isolates carrying CB4856-like *glc-1* alleles to N2 and CB4856 and measured the abamectin response of the F1 cross-progeny (Fig. 3D). F1 progeny from crosses of MY10, JU258, EG4350, and MY19 to N2 were sensitive,
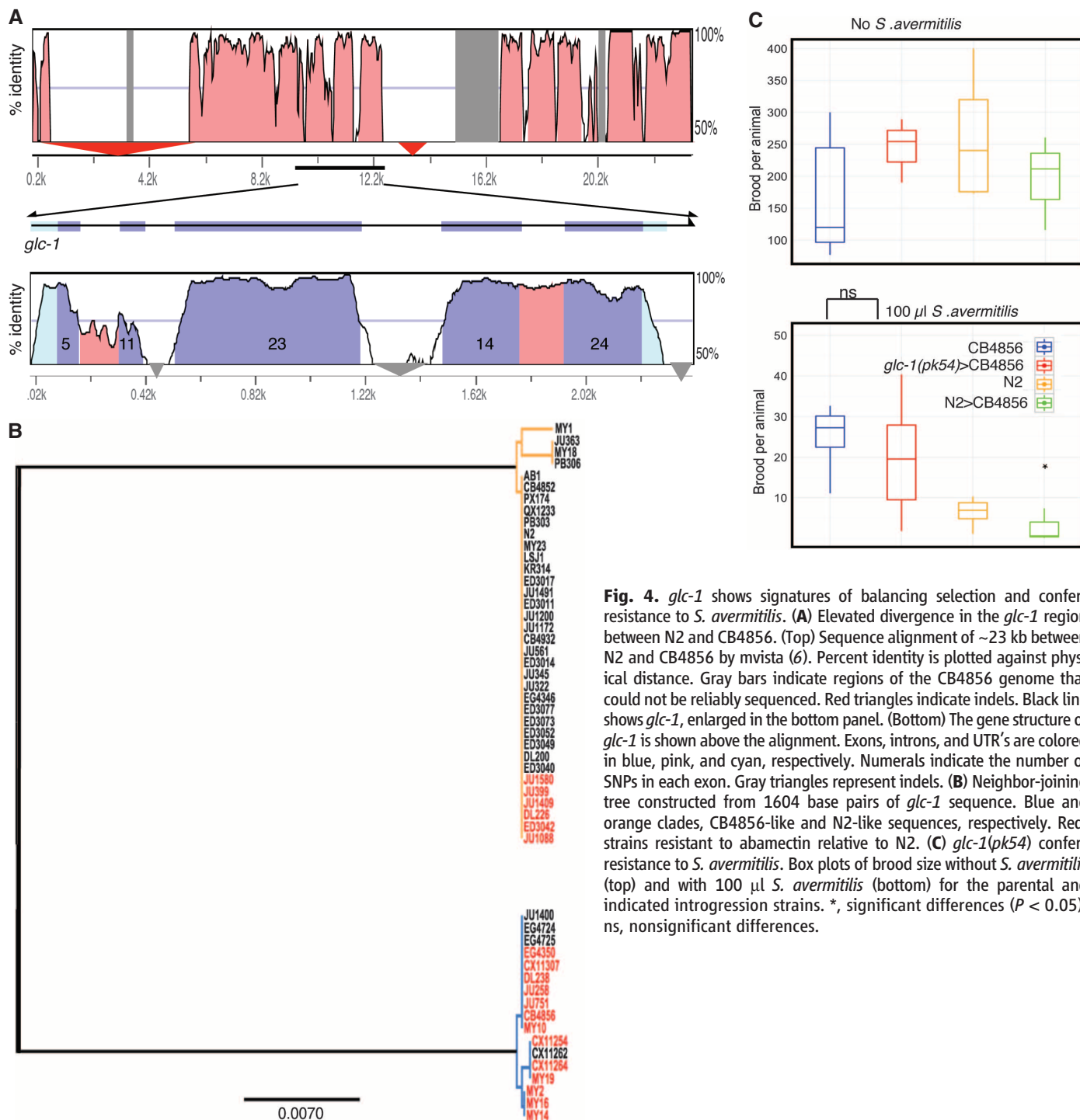

Fig. 4. *glc-1* shows signatures of balancing selection and confers resistance to *S. avermitilis*. (**A**) Elevated divergence in the *glc-1* region between N2 and CB4856. (Top) Sequence alignment of ~23 kb between N2 and CB4856 by mvista (6). Percent identity is plotted against physical distance. Gray bars indicate regions of the CB4856 genome that could not be reliably sequenced. Red triangles indicate indels. Black line shows *glc-1*, enlarged in the bottom panel. (Bottom) The gene structure of *glc-1* is shown above the alignment. Exons, introns, and UTR's are colored in blue, pink, and cyan, respectively. Numerals indicate the number of SNPs in each exon. Gray triangles represent indels. (**B**) Neighbor-joining tree constructed from 1604 base pairs of *glc-1* sequence. Blue and orange clades, CB4856-like and N2-like sequences, respectively. Red, strains resistant to abamectin relative to N2. (**C**) *glc-1(pk54)* confers resistance to *S. avermitilis*. Box plots of brood size without *S. avermitilis* (top) and with 100 μl *S. avermitilis* (bottom) for the parental and indicated introgression strains. *, significant differences ($P < 0.05$); ns, nonsignificant differences.

whereas F1 progeny from crosses of these isolates to CB4856 were resistant, consistent with abamectin resistance in these strains also arising from loss of *glc-1* function. However, F1 progeny from crosses of CX11307 and JU751 to both CB4856 and N2 were resistant, despite the same *glc-1* sequence, suggesting the presence of a second, dominant resistance factor in these isolates (Fig. 3D). Taken together, these results imply that variation in *glc-1* plays a major role in shaping abamectin resistance among *C. elegans* isolates, but the trait also involves other loci.

The *glc-1* region exhibited high sequence divergence between N2 and CB4856 (Fig. 4A), with 178 SNPs in ~5 kb, a polymorphism rate ~30 times higher than the genome-wide average of one SNP per 840 bases (*15*). Sequences of five other glutamate-gated chloride channel subunit genes differed very little between N2 and CB4856 (fig. S7B). Multiple lines of evidence suggested that the elevated level of polymorphism in *glc-1* is due to long-term balancing selection, rather than an elevated mutation rate or population subdivision. Elevated sequence diversity is not consistent with relaxed constraint on one *glc-1* allele, because the ratio of nonsynonymous to synonymous substitutions was 0.27, indicative of purifying selection (table S2). The *glc-1* sequences obtained from 53 wild isolates fall into two divergent clades (Fig. 4B). We observed 105 segregating sites among the isolates, but only six distinct haplotypes, fewer than expected for sequences evolving neutrally [$P < 0.0001$; (*6*), table S2]. The SNPs in the region surrounding *glc-1* were in complete linkage disequilibrium (fig. S9). We also observed a significant positive Tajima's D (*16*) (3.22; $P < 0.0001$) (table S2), which is expected under balancing selection. Population subdivision is unlikely to explain these observations because both N2-like and CB4856-like haplotypes are observed globally, without any apparent geographic structure (fig. S10). The extent of sequence divergence between the two haplotype clades was used to estimate that both haplotype classes have likely existed for 7.6×10^6 generations (*6*), which is older than typical coalescence times for neutral sequences in *C. elegans*. The observed molecular signatures in this region are analogous to the *zeel-1/peel-1* region involved in a genetic incompatibility, where two ancient, highly diverged haplotype clades are also maintained by balancing selection (*17*).

Because avermectins are metabolites of *S. avermitilis*, a ubiquitous soil bacterium (*1*), exposure to *S. avermitilis* may represent a selective force for this balancing selection. *S. avermitilis* significantly reduced the brood size (Fig. 4C and fig. S11) and induced uncoordinated movement in both CB4856 and N2. However, in the presence of *S. avermitilis*, the median brood size of CB4856 was about five times higher than N2. By contrast, in the absence of *S. avermitilis,* the median brood size of CB4856 was about

half that of N2 (Fig. 4C). The strain with the *glc-1* region from N2 introgressed into CB4856 showed a brood size reduction similar to N2 when exposed to *S. avermitilis*, whereas the introgression strain harboring the *glc-1(pk54)* mutation did not (Fig. 4C). These data are consistent with the hypothesis that a loss-of-function allele of *glc-1* in the CB4856 background is responsible for generating resistance to *S. avermitilis*, most likely through its effect on avermectin resistance. Thus, the CB4856 *glc-1* allele may confer resistance to *S. avermitilis* but reduce fitness in the absence of this bacterium, perhaps due to pleiotropy of *glc-1*. *glc-1* has been implicated in shaping the normal foraging pattern in N2 (*18*) and is likely to form heteromeric channels with other glutamate-gated chloride channel subunits (*2*, *3*, *19*) that are critical for multiple physiological processes (*3*, *20*). *glc-1* is expressed in multiple tissues from the embryo through the adult stage, consistent with a role in diverse biological functions (fig. S12).

Although diverse molecules have been identified as targets of avermectins (*3*), only a few studies have examined natural resistance, with glutamate-gated chloride channels implicated in some (*21*, *22*) but not others (*23*, *24*). We have identified a naturally occurring four-amino-acid deletion in the ligand-binding domain of GLC-1 that plays a major role in avermectin resistance in the global *C. elegans* population. In the standard laboratory N2 strain, loss of function of three distinct glutamate-gated chloride channel subunits is required for resistance to avermectins as measured both by growth (*13*) and by our swimming assay (fig. S4). In contrast, we show that the loss of function of one channel subunit is sufficient for resistance in some wild isolates. The observed differences in resistance are modest compared with those in some species (*25*), which suggests that other mechanisms may be involved in generating greater resistance. The *glc-1* variant that confers resistance to avermectins appears to be ancient and maintained by balancing selection, possibly due to a trade-off between resistance to common soil bacteria and a cost in their absence. Although we did not detect any obvious effect of this *glc-1* variant on brood size in laboratory conditions in the absence of *S. avermitilis*, it is possible that in the wild, the effect of a *glc-1* loss-of-function allele on multiple physiological processes may lead to lower fecundity or higher mortality. Analogous trade-offs have been observed for pathogen resistance genes in *Arabidopsis* (*26–28*). Because many nematodes, including parasitic ones, spend part of their life cycle in soil, resistance to avermectins in the phylum may be common.

References and Notes

1. R. W. Burg *et al.*, *Antimicrob. Agents Chemother.* **15**, 361 (1979).
2. S. McCavera, T. K. Walsh, A. J. Wolstenholme, *Parasitology* **134**, 1111 (2007).
3. A. J. Wolstenholme, A. T. Rogers, *Parasitology* **131** (suppl.), S85 (2005).
4. A. J. Wolstenholme, I. Fairweather, R. Prichard, G. von Samson-Himmelstjerna, N. C. Sangster, *Trends Parasitol.* **20**, 469 (2004).
5. J. S. Gilleard, R. N. Beech, *Parasitology* **134**, 1133 (2007).
6. Materials and methods are available as supporting material on *Science* Online.
7. J. P. Arena *et al.*, *J. Parasitol.* **81**, 286 (1995).
8. A. I. Njue, R. K. Prichard, *Parasitol. Res.* **93**, 419 (2004).
9. M. V. Rockman, L. Kruglyak, *PLoS Genet.* **5**, e1000419 (2009).
10. L. Kruglyak, E. S. Lander, *Genetics* **139**, 1421 (1995).
11. D. F. Cully *et al.*, *Nature* **371**, 707 (1994).
12. D. K. Vassilatis *et al.*, *J. Biol. Chem.* **272**, 33167 (1997).
13. J. A. Dent, M. M. Smith, D. K. Vassilatis, L. Avery, *Proc. Natl. Acad. Sci. U.S.A.* **97**, 2674 (2000).
14. R. E. Hibbs, E. Gouaux, *Nature* **474**, 54 (2011).
15. S. R. Wicks, R. T. Yeh, W. R. Gish, R. H. Waterston, R. H. Plasterk, *Nat. Genet.* **28**, 160 (2001).
16. F. Tajima, *Genetics* **123**, 585 (1989).
17. H. S. Seidel, M. V. Rockman, L. Kruglyak, *Science* **319**, 589 (2008).
18. A. Cook *et al.*, *Mol. Biochem. Parasitol.* **147**, 118 (2006).
19. A. Etter, D. F. Cully, J. M. Schaeffer, K. K. Liu, J. P. Arena, *J. Biol. Chem.* **271**, 16035 (1996).
20. J. A. Dent, M. W. Davis, L. Avery, *EMBO J.* **16**, 5867 (1997).
21. A. I. Njue, J. Hayashi, L. Kinne, X. P. Feng, R. K. Prichard, *J. Neurochem.* **89**, 1137 (2004).
22. D. H. Kwon, K. S. Yoon, J. M. Clark, S. H. Lee, *Insect Mol. Biol.* **19**, 583 (2010) (Aug).
23. A. El-Abdellati *et al.*, *Int. J. Parasitol.* **41**, 951 (2011).
24. S. McCavera, A. T. Rogers, D. M. Yates, D. J. Woods, A. J. Wolstenholme, *Mol. Pharmacol.* **75**, 1347 (2009).
25. R. M. Kaplan *et al.*, *Int. J. Parasitol.* **37**, 795 (2007).
26. M. Todesco *et al.*, *Nature* **465**, 632 (2010).
27. E. A. Stahl, G. Dwyer, R. Mauricio, M. Kreitman, J. Bergelson, *Nature* **400**, 667 (1999).
28. D. Tian, M. B. Traw, J. Q. Chen, M. Kreitman, J. Bergelson, *Nature* **423**, 74 (2003).

Supporting Online Material
www.sciencemag.org/cgi/content/full/335/6068/574/DC1
Materials and Methods
Figs. S1 to S12
Tables S1 and S2
References (*29–46*)